Korean J. Chem. Eng., **29**(2), 243-248 (2012)
DOI: 10.1007/s11814-011-0168-4

Morphology-controlled synthesis of CuO nano- and microparticles using microwave irradiation

Alum Jung, Seungho Cho, Won Joon Cho, and Kun-Hong Lee[†]

Department of Chemical Engineering, Pohang University of Science and Technology (POSTECH),
San 31, Hyoja-dong, Nam-gu, Pohang, Gyungbuk 790-784, Korea

(*Received 15 May 2011 • accepted 4 July 2011*)

Abstract−Microwave irradiation was used to obtain a variety of CuO crystal morphologies, including leaf-like, dandelion-like, and hollow structures. The morphology of the CuO crystals was controlled by varying the alkali source (NaOH, hexamethylenetetramine, ammonia, or urea) and heating at 95 °C for 1 hr. The X-ray diffraction patterns of as-prepared CuO crystals were consistent with high quality crystals with a monoclinic crystal structure. Field emission scanning electron microscopy (FE-SEM) and tunneling electron microscopy (TEM) images of CuO crystals revealed that the leaf-like CuO crystals had an average length of 950 nm and width of 450 nm, the small leaf-like CuO crystals had an average length of 450 nm and width of 200 nm, the dandelion-like CuO structures had an average diameter of 2 m, and the hollow CuO structures had an average diameter 2 m. Possible mechanisms for structure formation during the shape-selective CuO synthesis were proposed based on these results.

Key words: Hydrothermal Synthesis, Copper Oxide, Microwave, Ammonia, Urea

INTRODUCTION

As a p-type semiconductor with a narrow band gap (Eg=1.2 eV) [1], copper(II) oxide (CuO) has been widely investigated in diverse electronic, magnetic, and optical applications, such as heterogeneous catalysts, gas sensors, magnetic storage media, solar cells, optical switches, lithium ion battery anode materials, and field-emission emitters [2-8]. Recent studies demonstrated that CuO could exist in as many as three different magnetic phases [9], and it forms the basis for several high-temperature superconductors [10].

Because the properties of a crystal may be influenced by the crystal morphology, control of the size and morphology of CuO crystals becomes an attractive challenge. For example, Park et al. [11] reported that urchin-like CuO crystals exhibited excellent electrochemical performance for lithium-ion batteries, far superior to the performance of other morphologies. In response to the strong interest in control over shape and size, well-defined CuO nanostructures with different dimensionalities and shapes have been obtained [12-23].

Over the past few decades, CuO micro- and nanostructures have been prepared by a variety of synthetic approaches [24-29]. Among them, the hydrothermal process has been extensively used because of its low synthesis temperature and ease of scaling-up, although it requires a relatively long reaction time, typically 6-12 hours or more [30,31]. This problem can be alleviated by using microwave irradiation, which is a part of electromagnetic spectrum with frequencies ranging from 300 MHz to 300 GHz. The merits of microwave-assisted heating include rapid heating, low synthesis temperature, reduced processing time, increased product yield, energy savings, and environmental friendliness [32-34]. Moreover, we achieved high selectivity by rapidly traversing the intermediate temperature range during heating to the desired reaction temperature.

In the present work, we synthesized CuO crystals with different morphologies using a microwave hydrothermal method. The shapes of the CuO crystals were easily tuned by varying the alkali source, which supplied different quantities of hydroxide ions and ammonia molecules. A three-dimensional spherical structure was favored over the two-dimensional planar structure in the presence of ammonia. The results led us to propose a growth mechanism for achieving the shape-selective CuO crystals.

EXPERIMENTAL AND CHARACTERIZATION

1. Preparation of CuO Structures

As summarized in Table 1, four major synthetic conditions were used in the current work. All chemicals used were of analytical grade and were not purified further. CuO nanostructures were produced using copper nitrate ($Cu(NO_3)_2 \cdot 3H_2O$, 99%, Shinyou) as the copper cation precursor and hexamethylenetetramine (HMT, $(CH_2)_6N_4$, 99%, Junsei), sodium hydroxide (1 N, Samchun), ammonia (28.0-30.0 wt%, Junsei), or urea ($CO(NH_2)_2$, Aldrich) as the hydroxide anion source.

An aqueous solution (100 mL) composed of copper nitrate (1 mmol) and sodium hydroxide (1 mL) was prepared and stirred for 20 min at room temperature (Solution A, pH=7). After stirring, solution A was irradiated using a temperature-controlled microwave synthesis system (2.45 GHz, single-mode, Greenmotif, IDX, Japan) at 95 °C for 1 h. Subsequently, the irradiated solution was filtered using a polycarbonate membrane filter (ISOPORETM) with pores 100 nm in diameter. The black precipitate was washed several times with deionized (DI) water after filtration and dried in an oven. Solution B (pH=7) was prepared by adding 1 mmol HMT to deionized (DI) water (100 mL) containing copper nitrate (1 mmol). Solu-

---

[†] To whom correspondence should be addressed.
E-mail: ce20047@postech.ac.kr

Table 1. The detailed reaction condition and corresponding results

Sample	$Cu(NO_3)_2$	Alkali source	Time for stirring	Reaction condition	Morphology
A	1 mmol	NaOH 1 mmol	20 min	95 °C, 1 h	Leaf-like structure (~500 nm)
B	1 mmol	HMT 1 mmol	20 min	95 °C, 1 h	Leaf-like structure (~900 nm)
C	1 mmol	30 wt% Ammonia 4 mL	20 min	95 °C, 1 h	Dandelion-like structure
D	1 mmol	Urea 20 mmol		95 °C, 1 h	Hollow sphere structure

tion C (pH=11) was prepared by adding 4 mL ammonia to deionized (DI) water (96 mL) containing copper nitrate (1 mmol). Solution D (pH=6) was prepared by mixing copper nitrate (1 mmol) and urea (20 mmol) to form an aqueous solution (100 mL). As-prepared solutions B and C were submitted to the same treatment described for solution A. Solution D was submitted to the same treatment as well, but without the stirring time.

2. Characterization

Field emission scanning electron microscopy (FESEM, JEOL JMS-7400F, operated at 10 keV), high-resolution transmission electron microscopy (HRTEM, JEOL JEM-2100F with energy-dispersive X-ray spectrometry (EDX), operated at 200 kV), and X-ray diffraction studies (XRD, Mac Science, M18XHF) were used to observe the morphology, crystallinity, and chemical composition of the CuO structures.

RESULTS AND DISCUSSION

1. Crystal Structure of CuO

Fig. 1 shows FE-SEM images, TEM images, and selected-area electron diffraction (SAED) patterns of different shapes of the CuO structures obtained using different reagents in the microwave hydrothermal method. The leaf-like CuO nanostructures, synthesized in the sodium hydroxide (NaOH) solution, can be clearly observed in Fig. 1(a). The leaf-like CuO structures had an average length of 950 nm and width of 450 nm. Fig. 1(b) shows that CuO crystals obtained from the HMT solution displayed the same leaf-like shape but were smaller than the CuO crystals obtained from the NaOH solution. The CuO crystals obtained from the HMT solution had an average length of 450 nm and width of 200 nm. The dandelion-like CuO structures, synthesized from the ammonia solution, can be observed in Fig. 1(c). They were spherical structures with an average diameter of 2 μm, but they had extremely rugged surfaces due to the presence of densely packed flat sheets. Fig. 1(d) displays a hollow CuO structure, synthesized from the urea solution. The hollow structure of CuO has attracted great interest among synthetic chemists [35-37] for applications such as lithium ion battery anode materials [11, 38] due to its low density and large specific surface area [39]. In our work, hollow sphere CuO structures with an average diameter of 2 μm were synthesized by a fast, simple, and reproducible method that did not require templates, catalysts, or surfactants. The SAED patterns of these CuO structures (right bottom images of Fig. 1, panels (a), (b), and (c)) confirmed that they were single crystalline, whereas the hollow CuO (right bottom image of Fig. 1, panel (d)) crystals were polycrystalline.

XRD patterns of the as-prepared CuO crystals are shown in Fig.

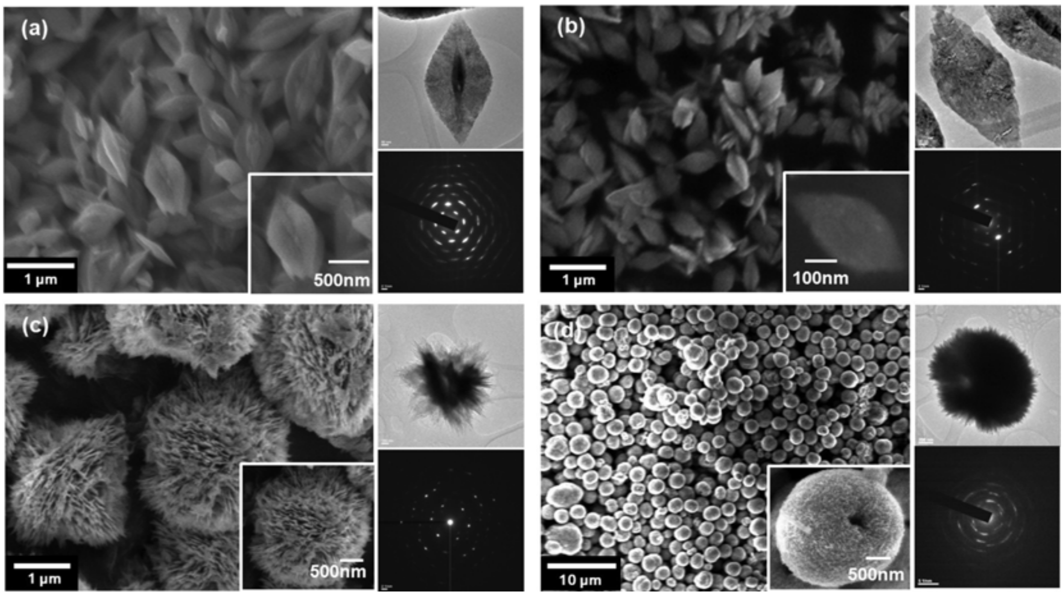

Fig. 1. Morphology and crystallinity (lower right) of the CuO structures synthesized by the microwave irradiation heating method: (a) leaf-like CuO structures synthesized in the presence of NaOH, (b) smaller leaf-like CuO structures synthesized in the presence of HMT, (c) spherical dandelion CuO structures synthesized in the presence of ammonia, (d) hollow spherical CuO structures synthesized in the presence of urea.

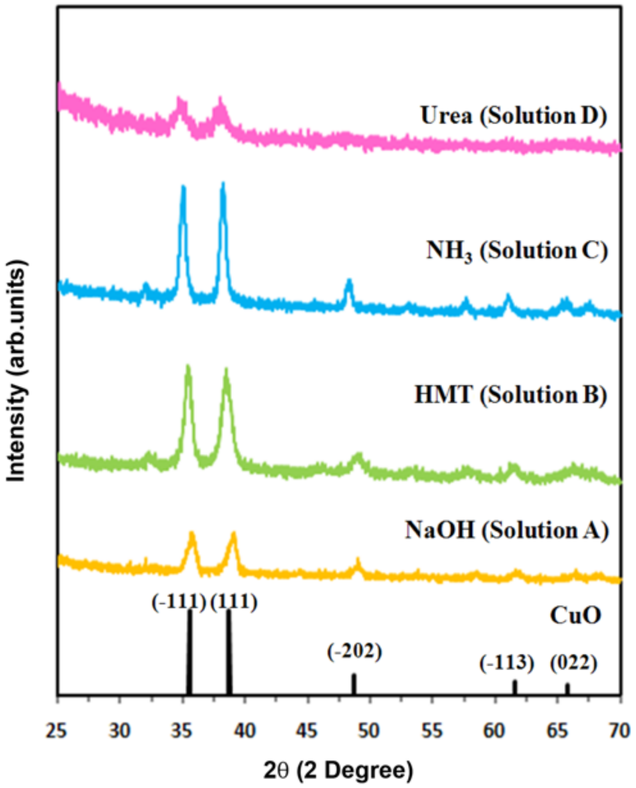

Fig. 2. Identification of CuO from XRD peaks collected from the CuO structures obtained by microwave irradiation.

2. All diffraction peaks were indexed in the CuO monoclinic phase (space group: C2/c, a=4.685 Å, b=3.425 Å, c=5.13 Å, β=99.549, JCPDS Card No. 41-0254). Peak broadening arose from the small size of the particles. Because no impurities were detected by XRD, it could be concluded that a single phase of CuO structures was successfully obtained through the microwave-assisted synthetic route.

2. Growth Mechanisms of the CuO Structure Formation

In general, CuO structures are believed to be obtained from the transformation of copper(II) hydroxide ($Cu(OH)_2$) during CuO synthesis. Supersaturation of the copper cations and hydroxide anions produces copper ion complexes, such as $[Cu(OH)_4]^{2-}$ or $[Cu(NH_3)_4]^{2+}$ [40,41], which are then converted to $Cu(OH)_2$ initial nuclei. The growth units attached to the nuclei stabilize the structures and increase the crystal size. CuO structures were obtained from the transformation of $Cu(OH)_2$ crystals under heat. Therefore, various shapes of CuO crystals were obtained by choosing different solutions and by controlling the concentrations of the precursors.

Figs. 3(a)-3(d) show a schematic illustration of the possible growth mechanisms of the CuO crystals from the NaOH, HMT, ammonia, and urea solutions, respectively. Fig. 3(a) illustrates the growth process of the CuO crystals synthesized from the NaOH solution. As a strong base, NaOH can supply hydroxide anions quickly. The relevant chemical reactions involved in CuO formation are believed to be the following [40]:

$$Cu^{2+}+4OH^{-}\rightarrow[Cu(OH)_4]^{2-} \quad (1)$$

$$[Cu(OH)_4]^{2-}\rightarrow Cu(OH)_2+2OH^{-} \quad (2)$$

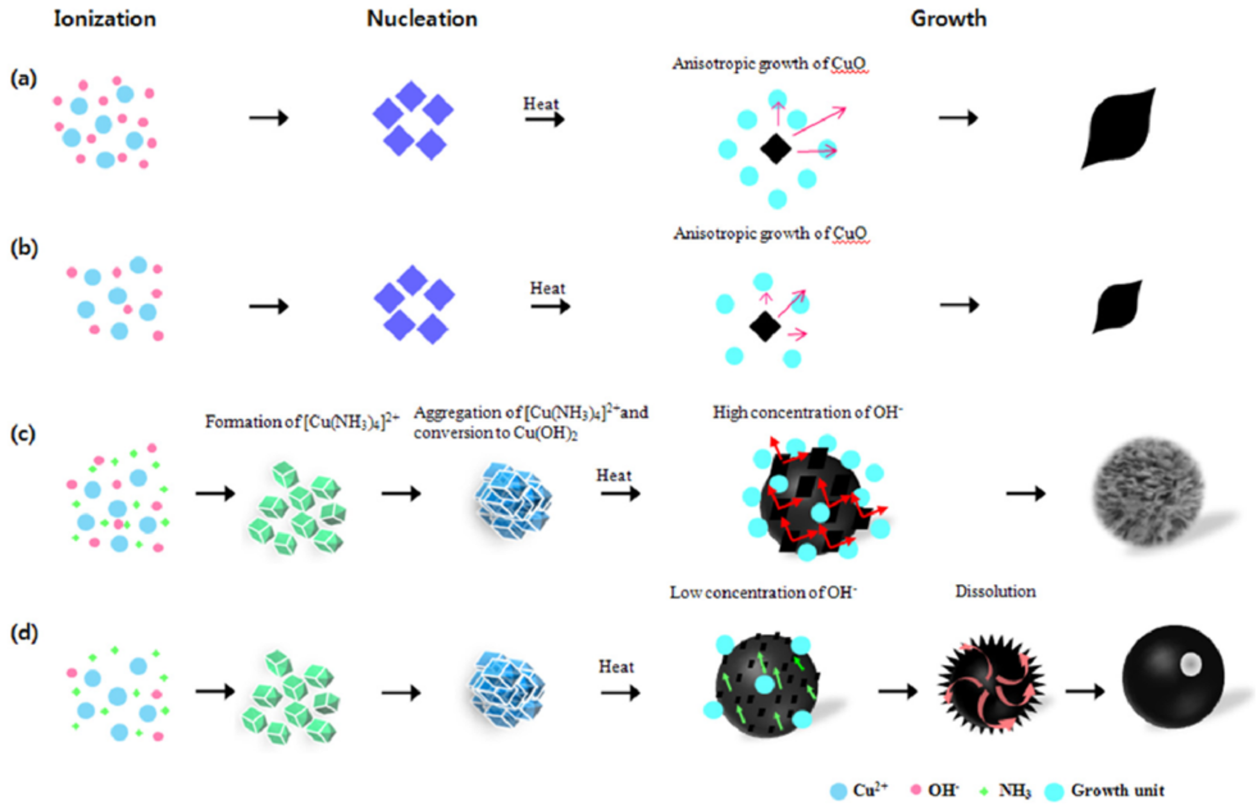

Fig. 3. Schematic diagram of the proposed formation mechanisms of the CuO structures: (a) leaf-like CuO structure synthesized in the presence of NaOH, (b) smaller leaf-like CuO structure synthesized in the presence of HMT, (c) spherical dandelion CuO structure synthesized in the presence of ammonia, (d) hollow sphere CuO structure synthesized in the presence of urea.

$$Cu(OH)_2 \rightarrow CuO + H_2O \quad (3)$$

Because NaOH is ionized in aqueous solutions, the copper(II) ion can form a two-dimensional square planar copper complex ($[Cu(OH)_4]^{2-}$) that converts to $Cu(OH)_2$ and CuO under heat. The two-dimensional leaf-like CuO structures resulted from the anisotropic growth rates of CuO crystals due to the different surface densities of copper atoms [42].

Fig. 3(b) suggests the possible formation mechanism of CuO structures in the HMT solution. As a pH buffer, HMT can supply small amounts of hydroxide anions slowly and constantly [43]. The chemical reactions involved in the formation of CuO from the HMT solution were the same as reactions (1)-(3). The CuO crystal leaf shape could be obtained from the HMT solution, but with smaller size particles. This was because the HMT solution included a lower concentration of hydroxide ions, which were a source that enabled crystal growth. However, CuO crystals, obtained from the HMT solution, had better crystallinity because of a slow supply of hydroxide ions.

A possible growth mechanism of micro-dandelion CuO crystals, obtained from the ammonia solution, is illustrated in Fig. 3(c). In the ammonia solution, it was possible to form two types of cupper ion complexes: $[Cu(OH)_4]^{2-}$ and $[Cu(NH_3)_4]^{2+}$. The chemical reactions involved in CuO formation in the presence of ammonia are believed to be the following [41]:

$$Cu^{2+} + 4NH_3 \rightarrow [Cu(NH_3)_4]^{2+} \quad (4)$$

$$[Cu(NH_3)_4]^{2+} + 4OH^- \rightarrow [Cu(OH)_4]^{2-} + 4NH_3 \quad (5)$$

$$[Cu(OH)_4]^{2-} \rightarrow Cu(OH)_2 + 2OH^- \quad (6)$$

$$Cu(OH)_2 \rightarrow CuO + H_2O \quad (7)$$

In our study, ammonia played a crucial role in the formation of three-dimensional CuO spheres. The copper complex $[Cu(NH_3)_4]^{2+}$ apparently formed due to the high concentration of precursors in the presence of ammonia molecules. This solution produced a higher degree of supersaturation, which destabilized the complexes. A comparison of the stability constants for the copper ion complexes, which are equilibrium constants for complex formation in solution, showed that $[Cu(NH_3)_4]^{2+}$ was less stable than $[Cu(OH)_4]^{2-}$ (The stability constant of the copper ion complex $[Cu(NH_3)_4]^{2+}$ was 12.4±0.3 (at 25 °C) [44], whereas that of the $[Cu(OH)_4]^{2-}$ complex was 15.5±0.1 (at 20 °C) [45].). Therefore, unstable $[Cu(NH_3)_4]^{2+}$ complexes aggregated to form three-dimensional spheres under unstable conditions. The effects of ammonia were confirmed by adding acid to the HMT solution. HMT slowly hydrolyzes to ammonia and formaldehyde in acidic environments [43], so the HMT solution contained ammonia under acidic conditions, which could form spherical structures. Fig. 4(a) shows a CuO crystal spherical shape that was formed by the aggregation of leaf-like CuO structures. Three-dimensional CuO spheres formed in the presence of ammonia, which was present in the acid added to the HMT solution. The formation of the micro-dandelion CuO structures could be explained by the presence of two types of complexes in water: a high degree of supersaturation indicated that $[Cu(NH_3)_4]^{2+}$, which is less stable than $[Cu(OH)_4]^{2-}$, aggregated to form a stable spherical seed structure, and each nucleus grew in a different direction via formation of $[Cu(OH)_4]^{2-}$ complex sheet structures.

Finally, a possible growth mechanism for the formation of hollow CuO crystal structures in the urea solution is illustrated in Fig. 3(d). The urea solution yields a constant supply of a small amount of hydroxide anions and can supply ammonia molecules by the reaction (8) [46]:

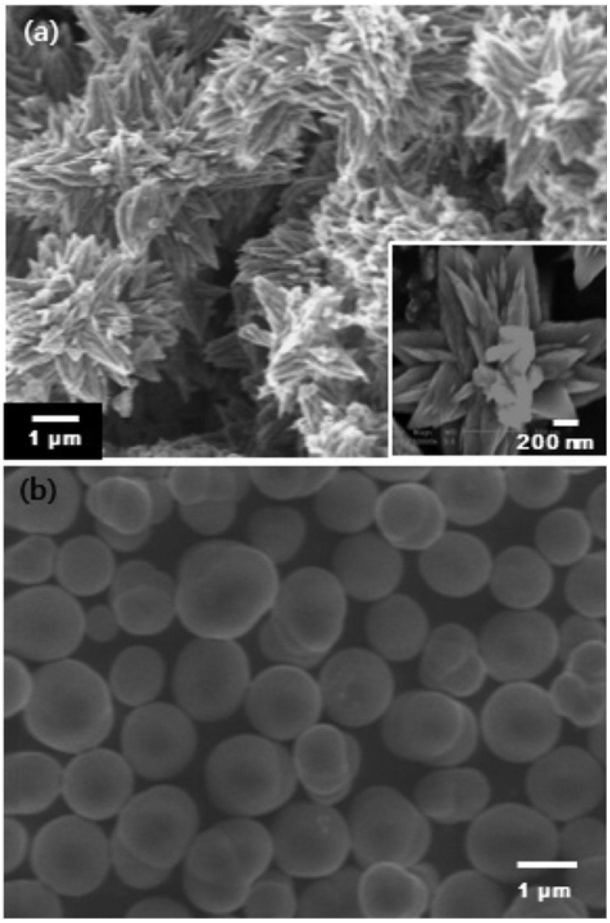

Fig. 4. Morphology of the CuO structures: (a) Aggregation of CuO crystals to form a three-dimensional spherical structure in the presence of ammonia; (b) CuO crystals obtained from a urea solution with a short reaction time (30 min).

$$xH_2O + NH_2CONH_2 \rightarrow 2NH_3 + CO_2 + (x-1)H_2O \quad (8)$$

The chemical reactions involved in the formation of CuO crystals in the urea solution are similar to the reactions (4)-(7). In the presence of ammonia supplied by the urea, a three-dimensional spherical shape can form. Each nucleus may then grow in a different direction by formation of small particles of $[Cu(OH)_4]^{2-}$ complexes on the spherical surface. This mechanism dominated because the urea solution supplied insufficient hydroxide anions to form two-dimensional sheet shapes in the CuO structures.

Many studies have investigated the formation of hollow CuO crystals, and a variety of synthesis methods have been developed. Two routes may be taken to obtain hollow CuO crystal structures: one route is CuO synthesis using surfactants, which form micelle structures [35], and the other route is formation of CuO aggregate particles near the interface between NH_3 gas bubbles and the liquid solution [36,37]. In this work, the hollow spheres apparently formed via dissolution of the spherical CuO surfaces after formation of CuO spherical structures. Fig. 4(b) shows SEM images of the CuO crystals obtained from urea solutions with a short reaction time (30 min). These images indicated that the spherical CuO crystals without a hollow structure were obtained before the hollow structure formed. Therefore, the spherical CuO structures first formed, followed by hollow structure formation via dissolution.

Particles synthesized in a urea solution by the conventional hydrothermal heating method are greenish copper hydroxynitrate ($Cu_2(OH)_3NO_3$) crystals. Hydroxide ions in solution, which are necessary for the synthesis of CuO crystals, can be supplied via urea decomposition at 60-100 °C, in the pH range of 5-7 [47]. The conventional hydrothermal method requires a lengthy heating process for the solution to reach 95 °C. During heating, the solution remains at a relatively low temperature for a long time, and very small quantities of hydroxide ions are present in solution due to the rare urea decomposition reaction. $Cu_2(OH)_3NO_3$ crystals are synthesized due to the lack of hydroxide ions. The $Cu_2(OH)_3NO_3$ crystals formed are converted to CuO crystals via the reaction (9) [48]:

$$Cu_2(OH)_3NO_3 \rightarrow 2CuO+HNO_3\,(g)+H_2O(g) \tag{9}$$

However, reaction (9) is extremely slow below 150 °C and becomes significant only above 250 °C [48]. Therefore, reaction (9) cannot occur and CuO crystals cannot be obtained via conventional hydrothermal heating.

In contrast, the microwave-assisted synthesis method heated the solution very quickly due to the rapid microwave heating. Because microwave heating reduced the heating time so that the urea decomposition temperature was reached quickly, there were fewer opportunities to make $Cu_2(OH)_3NO_3$, which forms in the presence of small quantities of hydroxide ions. CuO, therefore, could be obtained directly without the need to form the $Cu_2(OH)_3NO_3$ intermediate structure followed by conversion to CuO.

CONCLUSION

CuO crystalline leaf-like, dandelion-like, and hollow structures were successfully obtained via the microwave-assisted synthesis method. As-prepared CuO structures had a high crystallinity and uniform overall shape. Possible structure formation mechanisms for the shape-selective CuO synthesis were proposed based on the results. The key factor for controlling the shape of the CuO particles was the concentration of ammonia, which helped CuO crystals form three-dimensional spherical structures. In the presence of ammonia, three-dimensional spherical CuO crystals were obtained, possibly due to the aggregation of unstable $[Cu(NH_3)_4]^{2+}$ complexes. The quantities of hydroxide anions also influenced the size and surface morphology of the CuO crystals. The microwave-assisted hydrothermal synthesis method may be useful for achieving high selectivity in a product, especially if selectivity requires rapidly traversing an intermediate temperature range during heating to the desired reaction temperature.

ACKNOWLEDGEMENTS

This work was supported by grants from the second phase BK21 program of the Ministry of Education of Korea and the Korea Science and Engineering Foundation (KOSEF) grant funded by the Korean government (MEST) (Grant No. 2010-0000797).

APPENDIX A. SUPPLEMENTARY DATA

SEM images of the particles synthesized via conventional hydrothermal method at 95 °C for 1 h. XRD peak of the particle synthesized from the urea solution via conventional hydrothermal method at 95 °C, for 1 h.

REFERENCES

1. A. Q. Musa,T. Akomolafe and M. J. Carter, *Sol. Energy Mater. Sol. Cells*, **51**, 305 (1998).
2. J. B. Reitz and E. I. Solomon, *J. Am. Chem. Soc.*, **120**, 11467 (1998).
3. N. S. Baik, G. Sakai, N. Miura and N. Yamazoe, *J. Am. Ceram. Soc.*, **83**, 2983 (2000).
4. A. Chowdhuri, V. Gupta and K. Sreenivas, *Appl. Phys. Lett.*, **84**, 1180 (2004).
5. C. J. Barbe, F. Arendse, P. Comte, M. Jirousek, F. Lenzmann, V. Shklover and M. Gratzel, *J. Am. Ceram. Soc.*, **80**, 3157 (1997).
6. A. H. MacDonald, *Nature*, **414**, 409 (2001).
7. P. Poizot, S. Laruelle, S. Grugeon, L. Dupont and J. M. Tarascon, *Nature*, **407**, 496 (2000).
8. C. T. Hsieh, J.-M. Chen, H.-H. Lin and H.-C. Shih, *Appl. Phys. Lett.*, **83**, 3383 (2003).
9. (a) J. B. Forsyth, P. J. Brown and B. M. Wanklyn, *J. Phys. C: Solid State Phys.*, **21**, 2917 (1988). (b) B. X. Yang, T. R. Thurston, J. M. Tranquada and G. Shirane, *Phys. Rev. B*, **39**, 4343 (1989). (c) Y. P. Sukhorukov, N. N. Loshkareva, A. A. Samokhvalov, S. V. Naumov, A. S. Moskvin and A. S. Ovchinnikov, *J. Magn. Magn. Mater.*, **183**, 356 (1998).
10. (a) M. K. Wu, J. R. Ashburn, C. J. Torng, P. H. Hor, R. L. Meng, L. Gao, Z. J. Huang, Y. Q. Wang and C. W. Chu, *Phys. Rev. Lett.*, **58**, 908 (1987). (b) X. G. Zheng, C. N. Xu, Y. Tomokiyo, E. T. Tanaka, H. Yamada and Y. Soejima, *Phys. Rev. Lett.*, **85**, 5170 (2000).
11. J. C. Park, J. Kim, H. Kwon and H. Song, *Adv. Mater.*, **21**, 803 (2009).
12. H.-M. Xiao, S.-Y. Fu, L.-P. Zhu, Y.-Q. Li and G. Yang, *Eur. J. Inorg. Chem.*, 1966 (2007).
13. G. H. Du and G. V. Tendeloo, *Chem. Phys. Lett.*, **393**, 64 (2004).
14. Y. Zhang, S. Wang, X. Li, L. Chen, Y. Qian and Z. Zhang, *J. Cryst. Growth*, **291**, 196 (2006).
15. S. Li, H. Zhang, Y. Ji and D. Yang, *Nanotechnology*, **15**, 1428 (2004).
16. Y. Liu, Y. Chu, Y. Zhuo, M. Li, L. Li and L. Dong, *Cryst. Growth Design*, **7**, 3 (2007).
17. M. Zhang, X. Xu and M. Zhang, *Mater. Lett.*, **62**, 385 (2008).
18. Y. Zhang, S. Wing, X. Wang, T. Cui, W. Cui, Y. Zhang and Z. Zhang, *Eur. J. Inorg. Chem.*, 168 (2009).
19. M. A. Dar, Q. Ahsanulhaq, Y. S. Kim, J. M. Sohn, W. B. Kim and H. S. Shin, *Appl. Surface Sci.*, **255**, 6279 (2009).
20. S. Q. Wang, J. Y. Zhang and C. H. Chen, *Script. Mater.*, **57**, 337 (2007).
21. Y. Hu, X. Huang, K. Wang, J. Liu, J. Jiang, R. Ding, X. Ji and X. Li, *J. Solid State Chem.*, **183**, 662 (2010).
22. J. Zhu and X. Qian, *J. Solid State Chem.*, **183**, 1632 (2010).
23. W. Jia, E. Reitz, P. Shimpi, E. G. Rodriguez, P-X. Gao and Y. Lei, *Mater. Res. Bull.*, **44**, 1681 (2009).

24. J. T. Chen, F. Zhang, J. Wang, G. A. Zhang, B. B. Miao, X. Y. Fan, D. Yan and P. X. Yan, *J. Alloys and Compounds*, **454**, 268 (2009).
25. D. Barreca, A. Gasparotto, C. Maccato, E. Tondello, O. I. Lebedev and G. V. Tendeloo, *Cryst. Growth Design*, **9**, 2471 (2009).
26. M. Kaur, K. P. Muthe, S. K. Despande, S. Choudhury, J. B. Singh, N. Verma, S. K. Gupta and J. V. Yakhmi, *J. Cryst. Growth*, **289**, 670 (2006).
27. X. Zhang, D. Zhang, X. Ni and H. Zheng, *Solid-State Electronics*, **52**, 245 (2008).
28. C. Lu, L. Qi, J. Yang, D. Zhang, N. Wu and J. Ma, *J. Phys. Chem. B*, **108**, 17825 (2004).
29. K. R. Vijaya, R. Elgamiel, Y. Diamant, A. Gedanken and J. Norwig, *Langmuir*, **17**, 1406 (2001).
30. H.-M. Xiao, S.-Y. Fu, L.-P. Zhu, Y.-Q. Li and G. Yang, *Eur. J. Inorg. Chem.*, 1966 (2007).
31. S. Cho, S.-H. Jung and K.-H. Lee, *J. Phys. Chem. C*, **112**, 12769 (2008).
32. A. Loupy and L. Perreux, *Microwaves in organic synthesis*, Wiley-VCH, Weinheim, Germany (2002).
33. E. T. Thostenson and T.-W. Chou, *Composites: Part A*, **30**, 1055 (1999).
34. S. Das, A. K. Mukhopadhyay, S. Datta and D. Basu, *Bull. Mater. Sci.*, **32**, 1 (2009).
35. S. Wang, H. Xu, L. Qian, X. Jia, J. Wang, Y. Liu and W. Tang, *J. Solid State Chem.*, **182**, 1088 (2009).
36. S. Yang, C. Wang, L. Chen and S. Chen, *Mater. Chem. Phys.*, **120**, 296 (2010).
37. Y. Zhang, S. Wang, Y. Qian and Z. Zhang, *Solid State Sci.*, **8**, 462 (2006).
38. S. Gao, S. Yang, J. Shu, S. Zhang, Z. Li and K. Jiang, *J. Phys. Chem. C*, **112**, 19324 (2008).
39. (a) Y. D. Yin, Y. Lu, B. Gates and Y. N. Xia, *Chem. Mater.*, **13**, 1146 (2001). (b) M. Ohmori and E. Matijevic, *J. Colloid Interface Sci.*, **150**, 594 (1992).
40. G. H. Du and G. V. Tendeloo, *Chem. Phys. Lett.*, **393**, 64 (2004).
41. C. Lu, L. Qi, J. Yang, D. Zhang, N. Wu and J. Ma, *J. Phys. Chem. B*, **108**, 17825 (2004).
42. Z. Zhang, H. Sun, X. Shaom, D. Li, H. Yu and M. Han, *Adv. Mater.*, **17**, 42 (2005).
43. J. M. Dreyfors, S. B. Jones and Y. Sayed, *Am. Ind. Hyg. Assoc. J.*, **50**, 579 (1989).
44. L. N. Trevani, J. C. Roberts and P. R. Tremaine, *J. Solution Chem.*, **30**, 585 (2001).
45. E. Norkus and A. Vaskelis, *Polyhedron*, **13**, 3041 (1994).
46. J. N. Sahu, *J. Hazard. Mater.*, **164**, 659 (2009).
47. B. Mavis and M. Akinc, *J. Am. Ceram. Soc.*, **89**, 471 (2006).
48. C. Henrist, K. Traina, C. Hubert, G. Toussaint, A. Rulmont and R. Cloots, *J. Cryst. Growth*, **254**, 176 (2003).